

Received January 15, 2021; reviewed; accepted April 08, 2021

The intensified effect of nitrogen removal properties using *Pseudomonas fulva* K3 and MgBC for the weathered crust rare earth wastewater treatment

Xiangyi Deng¹, Ruan Chi^{1,2}, Chunqiao Xiao^{2,3}, Zhenyue Zhang¹, Xuemei Liu⁴, Jingang Hu³

¹ School of Resources and Safety Engineering, Wuhan Institute of Technology, Wuhan 430073, China

² Key Laboratory for Green Chemical Process of Ministry of Education, Wuhan Institute of Technology, Wuhan 430073, China

³ School of Environmental Ecology and Biological Engineering, Wuhan Institute of Technology, Wuhan 430205, China

⁴ School of Chemical Engineering and Pharmacy, Wuhan Institute of Technology, Wuhan 430205, China

Corresponding authors: rac_415@126.com (Ruan Chi), cqx_415@126.com (Chunqiao Xiao)

Abstract: A new bacteria named *Pseudomonas fulva* K3 (*P. fulva*) strain was isolated from the surroundings of weathered crust rare earth tailing with efficient $\text{NH}_4^+\text{-N}$ removal ability via heterotrophic nitrification and aerobic denitrification. The nitrogen removal properties could be intensified by the synergistic effect between as-prepared magnesium-modified biochar (MgBC) and *P. fulva* strain. The results show that *P. fulva* exhibited a rod-shaped morphology and $\text{NH}_4^+\text{-N}$ can be completely biodegraded under the optimal conditions of $\text{pH}=7.0\sim 8.0$, temperature $30\text{ }^\circ\text{C}$ and initial $\text{NH}_4^+\text{-N}$ concentration of $100\sim 150\text{ mg/L}$. The $\text{NH}_4^+\text{-N}$ tolerant concentration for *P. fulva* was determined to be 300 mg/L . The magnesium-modified biochar (MgBC) worked as an adsorbent of $\text{NH}_4^+\text{-N}$. The kinetics and isotherm model for adsorption could be described by the pseudo-second-order kinetic and Freundlich model, respectively. The XPS results showed that $\text{NH}_4^+\text{-N}$ was mainly adsorbed on the surface by chemical adsorption. Furthermore, the *P. fulva* could be immobilized on MgBC due to its large surface area, adjusting the concentration of $\text{NH}_4^+\text{-N}$ to a proper range for the growth of *P. fulva* by adsorption and desorption equilibrium, and leading to the intensified effect on nitrogen removal. The total nitrogen removal efficiency of the eluted weathered crust rare earth tailing reached 84.7% in MgBC + *P. fulva* system.

Keywords: weathered crust rare earth wastewater, nitrogen removal, pseudomonas fulva K3, magnesium-modified biochar, intensified effect

1. Introduction

Weathered crust rare earth ore is a crucial metal resource in the world, which contains large amounts of middle and heavy rare earth elements (He et al., 2016; Zhang et al., 2016a). More and more attention has been paid to the exploration and environmental protection due to its important role in economics and industries, such as luminescent materials, permanent magnet materials, rechargeable batteries, petrochemicals and metallurgical machinery et al. (Dutta et al., 2016). The rare earth elements exist as hydroxyl aqueous ions adsorbed on the clay minerals, resulting in the ion-exchange method as its recovery technology in industry (Zhou et al., 2019). And ammonium salts are widely used as leaching agents for the extraction of rare earth elements by in-situ leaching process (Feng et al., 2018; Wu et al., 2020; Zhao et al., 2017). Quite amounts of ammonia nitrogen ($\text{NH}_4^+\text{-N}$) is still remained in the ore body after the extraction process and it can be easily eluted by the rain, flowing into surface water and causing eutrophication (Li et al., 2017). It is of great significance to find an eco-friendly and effective method for the removal of $\text{NH}_4^+\text{-N}$ wastewater eluted from weathered crust rare earth tailing.

Several methodologies including blow-off, adsorption (Kizito et al., 2015), chemical precipitation (Huang et al., 2010), and biological technique (Ma et al., 2017b) have been mainly developed for the treatment of $\text{NH}_4^+\text{-N}$ wastewater. Compared with the physical and chemical removal methods, biological technique has the advantages of low cost, high security, and environmental friendliness (Zhang et al., 2019b). The existing conventional biological processes, such as A/O, A²/O, SBR, and MBR, are established on activated sludge and biofilm (Ahmad et al., 2017; Gong et al., 2018; Luo et al., 2017; Shams et al., 2018). $\text{NH}_4^+\text{-N}$ is firstly oxidized to $\text{NO}_2^-\text{-N}$ and $\text{NO}_3^-\text{-N}$ by autotrophic ammonia oxidizing bacteria (AOB) and nitrite oxidizing bacteria (NOB), respectively (Zhang et al., 2019a). Then the $\text{NO}_2^-\text{-N}$ and $\text{NO}_3^-\text{-N}$ are reduced to N_2 by heterotrophic denitrifying bacteria under anaerobic condition. However, the key factors limiting the industrial application of conventional biological method are the low nitrogen removal speed, tedious procedures and high energy consumption. Given those disadvantages of conventional biologic process, some new techniques are proposed to reduce the route and cost, such as shot cut nitrification-denitrification (Hou et al., 2017), anaerobic ammonium oxidation (Kosugi et al., 2020 ; Jia et al. 2017) and heterotrophic nitrification aerobic denitrification (HNAD) (An et al., 2020; Yang et al., 2017).

As a new species of bacteria discovered in recent years, the HNAD combines the heterotrophic nitrification ($\text{NH}_4^+ \rightarrow \text{NO}_2^-$ or NO_3^-) and simultaneous denitrification (NO_2^- or $\text{NO}_3^- \rightarrow \text{N}_2\text{O}$ or/and N_2) under aerobic conditions in a single bioreactor (Li et al., 2015). Thus, the route of nitrogen removal process is remarkably cut down and the $\text{NH}_4^+\text{-N}$ removal efficiency is much higher than that of conventional biological process due to its rapid proliferation. The increasing species of HNAD have been found and reported, such as *Enterobacter cloacae* CF-S27 (Padhi et al., 2017), *Pseudomonas Stutzeri* SDU10 (Chen et al., 2020), and *Acinetobacter* sp. Y16 (Huang et al., 2013). The eluted wastewater from the weathered crust rare earth tailing possesses the characteristics of high $\text{NH}_4^+\text{-N}$ concentration and low pH in which HNAD bacteria survived can be screened out with the highly efficiency for $\text{NH}_4^+\text{-N}$ removal (Wang et al., 2016).

The loss of HNAD bacteria in suspended treatment system is another obstacle factor for stable application. And carrier immobilization is an effective method to enhance biodegradation efficiency and reduce loss of microbes (Lü et al., 2019; Yuan et al., 2015). Many materials such as activated carbon, porous glass, alginate and biochar have been applied as the immobilization carrier (Banerjee et al., 2019; Talha et al., 2018). Compared with other carriers, biochar has the advantages of easy modification, nontoxicity, good availability, and low cost. In addition, biochar-based carrier has higher mass transport of oxygen and nutrients to accelerate the growth of bacteria (Zhang et al., 2016). The immobilization of HNAD on the biochar can promote the bacteria concentration in the system and the complex of HNAD and biochar can be reused, showing a promising rapid method for $\text{NH}_4^+\text{-N}$ removal. Isolating the efficient HNAD bacteria and immobilizing it on a biochar carrier that can also adsorb $\text{NH}_4^+\text{-N}$ is an important feasible strategy, but few researches have been reported.

In this work, a novel HNAD strain named *Pseudomonas fulva* K3 (*P. fulva*) with high $\text{NH}_4^+\text{-N}$ removal efficiency was isolated from surroundings of the weathered crust rare earth tailing. And the characteristics of nitrogen removal was investigated. The magnesium-modified biochar (MgBC) was prepared as an adsorbent of $\text{NH}_4^+\text{-N}$ and a carrier for *P. fulva* strain via thermal decomposition under oxygen-limited condition. The kinetics and isotherm of $\text{NH}_4^+\text{-N}$ adsorption was established. And the mechanism of the intensified effect of MgBC on the *P. fulva* was proposed by using BET, SEM, and XPS, providing a new strategy for $\text{NH}_4^+\text{-N}$ wastewater eluted from weathered crust rare earth ore.

2. Materials and methods

2.1. Preparation of MgBC

The corncobs used as biomass char precursor were collected from Hubei Province of China. The MgBC was prepared by the following steps: Firstly, the corncobs were dried and crushed to -2 mm particle size. Then the corncob was impregnated by 5.0 g/L NaOH solution for 12 h to remove impurities and introduced hydroxyl on the surface of corncob biomass. And the obtained corncob was washed with distilled water several times to neutral, followed by filtering and drying at 70 °C overnight. Secondly, the as-prepared corncob was immersed by 0.3 mol/L magnesium chloride solution for 4 h with stirring. Finally, the magnesium-bearing corncob was dried at 70 °C for 8 h and decomposed at 450 °C for 2 h

under anaerobic environment to obtain MgBC. The biochar without modification (BC) was prepared under identical conditions without the addition of magnesium.

2.2. Cultivation of *P. fulva* strain

P. fulva strain was separated from soil sample around the weathered crust rare earth tailing with ammonia nitrogen pollution, and cultivated using basal medium in 50 mL conical flask. The basal medium components for *P. fulva* enrichment were as follows: 5.0 g/L sodium citrate ($\text{Na}_3\text{C}_6\text{H}_5\text{O}_7 \cdot 2\text{H}_2\text{O}$), 0.47 g/L $(\text{NH}_4)_2\text{SO}_4$, 1.0 g/L K_2HPO_4 , 2.0 g/L NaCl, 0.5 g/L $\text{MgSO}_4 \cdot 7\text{H}_2\text{O}$, 0.01 g/L MnSO_4 , 0.04 g/L $\text{FeSO}_4 \cdot 7\text{H}_2\text{O}$. The basal medium was autoclaved for 20 min at 121 °C before cultivation. All reagents used in this work were of analytical reagent grade and purchased from Sinopharm Chemical Reagent Co., Ltd., Shanghai, China.

2.3. $\text{NH}_4^+\text{-N}$ removal performance of *P. fulva* strain

The $\text{NH}_4^+\text{-N}$ removal performance was investigated by batches of conical flask experiments. Briefly, the experimental medium was prepared by changing carbon source, the ratio of carbon to nitrogen (C/N), pH, and $\text{NH}_4^+\text{-N}$ concentration on the basis of basal medium. The OD_{600} value of enriched *P. fulva* solution in logarithmic phase was adjusted to 1.0 with sterile water. And 2.0 % (v/v%) of enriched *P. fulva* solution was inoculated into 50 mL medium in a 100 mL conical flask. The conical flask was transferred in a shaker at different rotate speed and temperature. The samples were obtained at intervals to determine OD_{600} and then centrifuged at 10000 r/min for 10 min. The supernatant was collected to measure the concentrations of $\text{NH}_4^+\text{-N}$, nitrite nitrogen ($\text{NO}_2^-\text{-N}$), nitrate nitrogen ($\text{NO}_3^-\text{-N}$), and total nitrogen (TN). The $\text{NH}_4^+\text{-N}$ biodegradation efficiency of *P. fulva* was obtained by subtracting the amount of gaseous ammonia generated in alkaline condition.

2.4. $\text{NH}_4^+\text{-N}$ adsorption properties of MgBC

The $\text{NH}_4^+\text{-N}$ adsorption experiments were carried out in 100 mL conical flasks containing 50 mL of the as-prepared medium. Then 1.0 % (wt.%) of MgBC powder was added into the conical flask, followed by transferring them to a shaker at 160 r/min at different temperature. After adsorption process, the sample was filtered by 0.22 μm filter membrane. The supernatant was collected to measure the concentration of $\text{NH}_4^+\text{-N}$, and the MgBC adsorbed by $\text{NH}_4^+\text{-N}$ was washed with distilled water and then dried for the subsequent characterization.

Equation (1) can be used to calculate the equilibrium adsorption amount (q_e) of MgBC (Ma et al. 2017a):

$$q_e = (C_0 - C_e) \cdot V/M \quad (1)$$

where C_0 (mg/L) and C_e (mg/L) are the initial and equilibrium adsorption concentration of $\text{NH}_4^+\text{-N}$, V (L) is the volume of the solution, and M (g) is the mass of MgBC powder.

2.5. Intensified effect of MgBC on *P. fulva* strain for $\text{NH}_4^+\text{-N}$ removal

The intensified effect of MgBC on *P. fulva* strain was investigated by adding both *P. fulva* and MgBC powder in $\text{NH}_4^+\text{-N}$ containing medium. 2.0 % (v/v%) of enriched *P. fulva* solution was inoculated into the medium, and then 1.0 % MgBC powder (wt.%) was added into the conical flask immediately. The samples were taken out periodically to test the concentration of $\text{NH}_4^+\text{-N}$. The residue after $\text{NH}_4^+\text{-N}$ removal process was washed and dried for the subsequent characterization. All experiments were repeated in triplicate.

2.6. Analytical methods and characterization

The concentrations of $\text{NH}_4^+\text{-N}$, $\text{NO}_3^-\text{-N}$ and $\text{NO}_2^-\text{-N}$ and TN were measured via Nessler's Reagent, ultraviolet spectrophotometry, N-1-naphthylethylenediamine dihydrochloride and potassium persulfate by using UV-vis spectrophotometer (UV-2600, Shimadzu, Kyoto, Japan), respectively. The absorbance at 600 nm (OD_{600}) was monitored to indicate the growth of *P. fulva* strain.

The microstructure of *P. fulva* strain and magnesium-modified biochar were observed by scanning electron microscopy (SEM, JSM-7001F, Shimadzu, Kyotocity, Japan). Especially, the *P. fulva* bacteria solution was centrifuged at 10000 r/min for 10 min, and then washed by distilled water three times. The pentanediol (2.5 % by v/v%) was used to immobilize the bacteria at 4 °C for 24 h. Then the *P. fulva* strain was dehydrated in an ascending serious concentration of ethanol (50%, 70%, 90%, and 100% by v/v%) for 10 min each time, followed by the displacement process with isoamyl acetate for 15 min. Lastly, the *P. fulva* strain was freeze-dried for SEM.

The surface area of biochar samples was measured using Brunauer-Emmett-Teller (BET, Micromeritics ASAP 2460, USA) method through N₂ adsorption isotherms. The X-ray photoelectron spectroscopy (XPS, Thermo Fischer ESCALAB 250Xi, USA) measurements were performed to detect the element valence states of MgBC before and after NH₄⁺-N adsorption process.

3. Results and discussion

3.1. NH₄⁺-N biodegradation characteristics of *P. fulva* strain

3.1.1. Morphology of *P. fulva* strain and growth characteristic

The morphology of *P. fulva* strain was observed by SEM. As shown in Fig. 1(A), the *P. fulva* isolated from soil sample around the weathered crust rare earth tailing was a rod-shaped bacterium with an average length of 1.8 μm. The growth of *P. fulva* strain was exhibited by recording OD₆₀₀ values in basal medium during biodegradation process. According the results shown in Fig. 1(B), Slogistic model was used to describe the growth curve of *P. fulva* strain. The equation of Slogistic model could be described as follows(Chen et al., 2016):

$$y(t) = a/(1 + b \cdot e^{-kx}) \quad (2)$$

where a, b, and k are constants of Slogistic model.

The R² of the fitting curve was 0.991, revealing that *P. fulva* strain could be adequately described the growth characteristic of *P. fulva* strain. The OD₆₀₀ increased significantly from 0.18 to 1.33 with the increasing time from 4 to 8 h and then remained stable afterward, indicating that the nutrient substances were almost exhausted and *P. fulva* strain reached stationary phase.

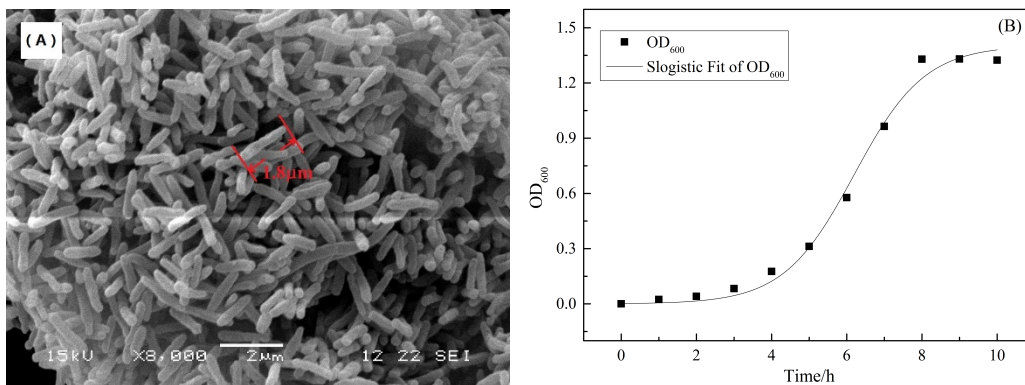


Fig. 1. Scanning electron microscopy images (SEM) (A) and growth curve (B) of *P. fulva* strain

3.1.2. The effect of initial pH on the ammonium biodegradation

The effects of initial pH on the OD₆₀₀ of *P. fulva* strain and the NH₄⁺-N biodegradation efficiency were investigated under the conditions of temperature of 30 °C, rotate speed of 160 r/min, and initial ammonia concentration of 100 mg/L. According to the results shown in Fig. 2, the initial pH is a significant factor during the biodegradation process. The OD₆₀₀ increases with the biodegradation time (Fig. 2(A)). The maximum (around 1.33) OD₆₀₀ could be reached under the conditions of pH=7.0, 8.0 and 9.0 at the biodegradation time of 8, 9, and 10 h, respectively. the growth of *P. fulva* strain was severely inhibited in strong acidic environment (pH<5.0) and slightly inhibited in alkaline environment (pH>10.0). As shown in Fig. 2(B), the effect of pH on NH₄⁺-N biodegradation rate was consistent with that of OD₆₀₀. The NH₄⁺-N can be completely removed in neutral and alkaline condition (pH=6.0~10.0),

and the maximum $\text{NH}_4^+\text{-N}$ biodegradation rate could be obtained at $\text{pH}=7.0$. The $\text{NH}_4^+\text{-N}$ is existed as ionic form in strong acidic environment, resulting in the unavailability for ammonia monooxygenase (Amo) in *P. fulva* strain. As pH increases, more molecular ammonia nitrogen was generated. Therefore, the biodegradation efficiency increases with the increasing pH value. However, the charge of cell membrane can be destroyed by excessive hydroxyl, leading to the decrease of $\text{NH}_4^+\text{-N}$ biodegradation efficiency.

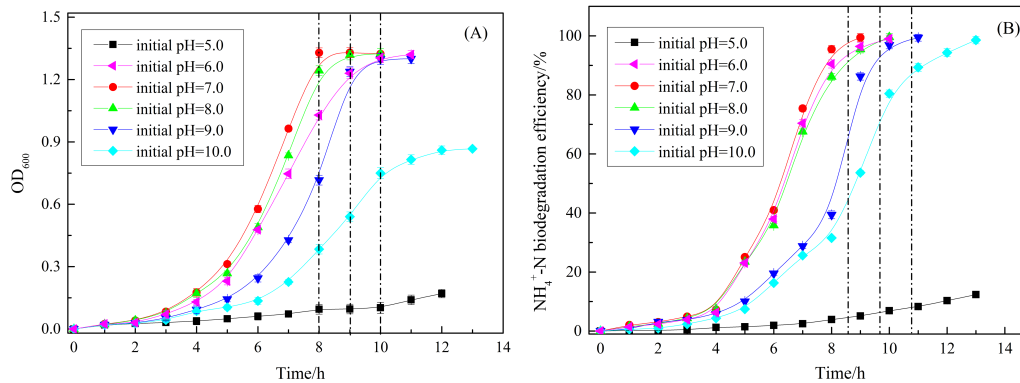


Fig. 2. The effect of initial pH on OD_{600} (A) and $\text{NH}_4^+\text{-N}$ biodegradation efficiency (B)

3.1.3. The effect of temperature on the ammonium biodegradation

The structure of bacteria, enzyme activity, substance transferring, and protein synthesis can be greatly impacted by temperature and further influence the $\text{NH}_4^+\text{-N}$ biodegradation. Fig. 3 exhibited the effect of temperature on $\text{NH}_4^+\text{-N}$ biodegradation efficiency under the conditions of $\text{pH}=7.0$, rotate speed of 160 r/min, and initial $\text{NH}_4^+\text{-N}$ concentration of 100 mg/L. The $\text{NH}_4^+\text{-N}$ biodegradation efficiency could be significantly influenced by temperature. The $\text{NH}_4^+\text{-N}$ biodegradation increased with the the increase of temperature ranging from 20 to 30 °C due to the improvement of enzyme activity and the diffusivity of substances, and then decreased in the range of 30 to 40 °C because of the denaturation of enzymes and proteins. The time of biodegradation for *P. fulva* was shortest at the temperature of 30 °C, indicating that the *P. fulva* strain could grow well for $\text{NH}_4^+\text{-N}$ removal.

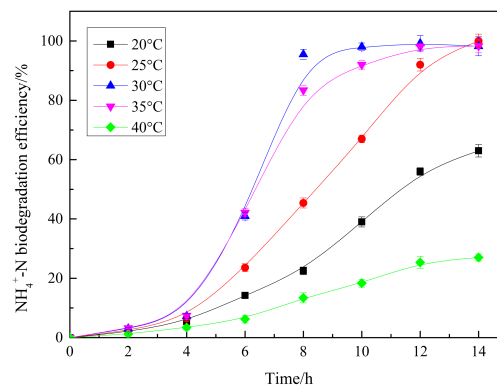


Fig. 3. The effect of temperature on $\text{NH}_4^+\text{-N}$ biodegradation efficiency

3.1.4. The effect of initial $\text{NH}_4^+\text{-N}$ concentration on ammonium biodegradation

The effect of initial $\text{NH}_4^+\text{-N}$ concentration (50~300 mg/L) on ammonium biodegradation was shown in Fig. 4. From the results in Fig. 4(A), the biodegradation time for $\text{NH}_4^+\text{-N}$ removal increased from 7 h to 60 h with the increasing $\text{NH}_4^+\text{-N}$ concentration from 50 mg/L to 300 mg/L. As shown in Fig. 4(B), the maximum removal rate of 34.51 mg/L/h was obtained under the initial $\text{NH}_4^+\text{-N}$ concentration of 150 mg/L, which was much higher than some reported researches, such as *Pseudomonas mendocina* X49 with a 26.39 mg/L/h maximum rate (Xie et al., 2021), and *Pseudomonas* sp. ADN-42 with a 11.6 mg/L/h maximum rate (Jin et al., 2015). In addition, the $\text{NH}_4^+\text{-N}$ maximum removal rates firstly increased (initial $\text{NH}_4^+\text{-N}$ concentration=50~150 mg/L) and then decreased (initial $\text{NH}_4^+\text{-N}$ concentration 200~300

mg/L). And the time for corresponding maximum removal rate shifted from 4 h to 12 h, indicating that the initial $\text{NH}_4^+\text{-N}$ concentration higher than 200 mg/L could burden the load of $\text{NH}_4^+\text{-N}$ and inhibit the growth of *P. fulva* strain.

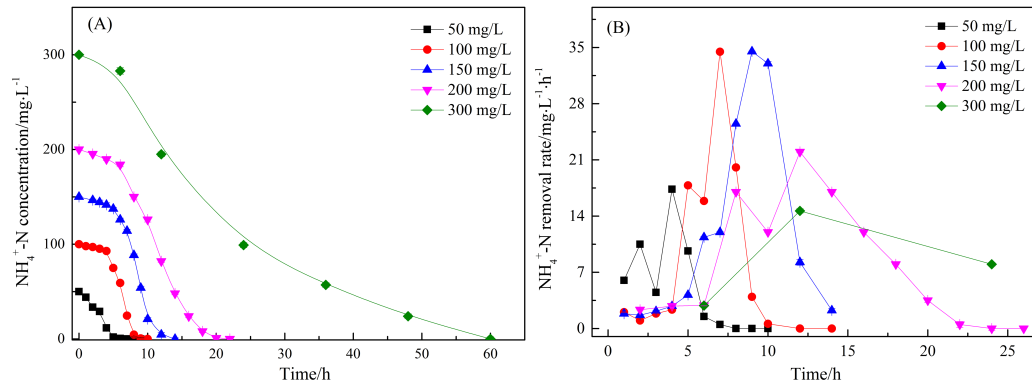


Fig. 4. The effect of initial $\text{NH}_4^+\text{-N}$ on biodegradation process

3.2. $\text{NH}_4^+\text{-N}$ adsorption behaviors of MgBC

3.2.1. Characterization of BC and MgBC

Fig. 5(A) and Fig. 5 (B) displayed the SEM images of BC and MgBC, respectively. The morphology of BC changed remarkably after modified by magnesium. The biochar without modification were observed to be composed of small knots with layer structure, and the surface was quite smooth. While the magnesium-modified biochar exhibited a relatively rougher surface due to the pyrolysis decomposition of MgCl_2 . The N_2 adsorption isotherm curve of MgBC measured by BET is shown in Fig. 5(C). The specific surface area of as-prepared MgBC is $6.37 \text{ m}^2/\text{g}$ with an adsorption average pore diameter of 8.50 nm (the inset of Fig. 5(C)), providing a large amount of adsorption sites for $\text{NH}_4^+\text{-N}$ and *P. fulva* bacteria. The EDS result of the MgBC is shown in Fig. 5(D). The appearance of Mg element reveals that the biochar is successfully modified by Mg.

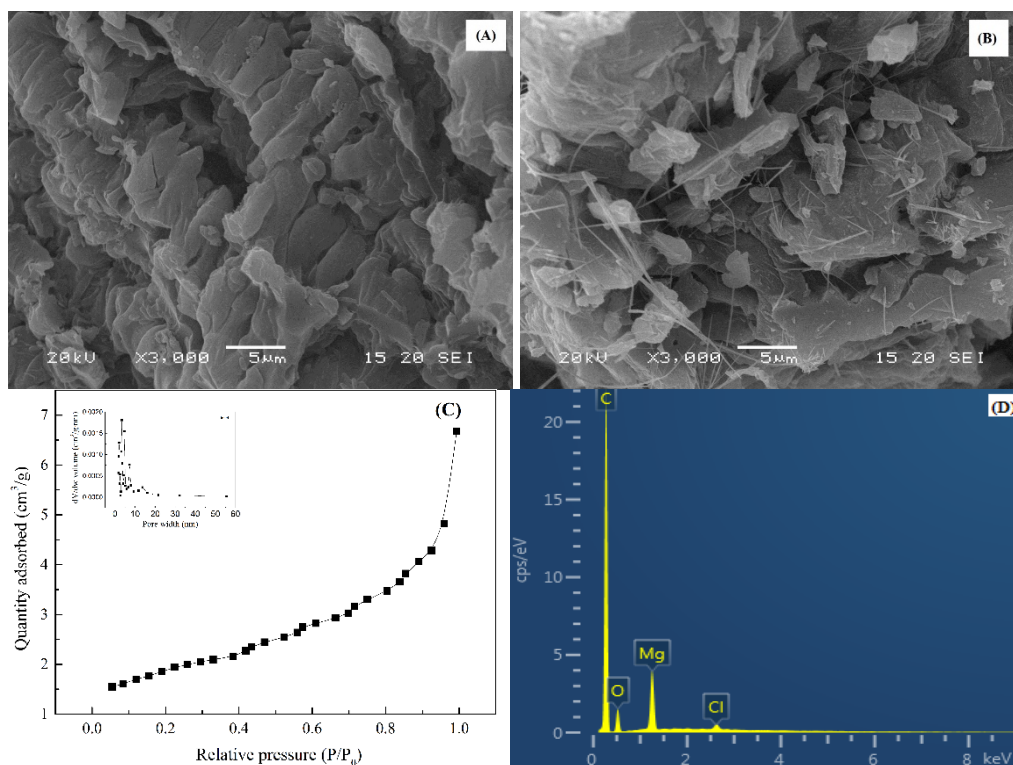


Fig. 5. The SEM images of BC(A), and MgBC(B), N_2 adsorption isotherm curve of MgBC (C), EDS of MgBC (D)

3.2.2. $\text{NH}_4^+\text{-N}$ adsorption kinetics and isotherms

Two kinetic models, namely Lagergren's pseudo-first-order model (Eq. 3) and pseudo-second-order kinetic model (Eq. 4), were used to study the adsorption behaviors of MgBC (Li et al. 2019). And the equations are expressed as follows:

$$\ln(q_e - q_t) = -K_1 t + \ln q_t \quad (3)$$

$$\frac{1}{q_t} = \frac{1}{K_2 q_e^2 t} + \frac{1}{q_e} \quad (4)$$

where q_t ($\text{mg}\cdot\text{g}^{-1}$) and q_e ($\text{mg}\cdot\text{g}^{-1}$) are the amount of the adsorbed $\text{NH}_4^+\text{-N}$ at time t (min) and at equilibrium, K_1 (min^{-1}) and K_2 (min^{-1}) are the adsorption rate constant of the pseudo-first-order equation and pseudo-second-order equation.

The $\text{NH}_4^+\text{-N}$ adsorption kinetics were carried out in basal medium under the conditions of initial $\text{NH}_4^+\text{-N}$ concentration of 100 mg/L, temperature of 30 °C, and the MgBC dosage of 1.0 % (wt%). The equilibrium was achieved within 180 min with a maximum adsorption capacity of 2.23 mg/g. The adsorption kinetics models fitted by pseudo-first-order model and pseudo-second-order model were exhibited in Fig. 6(A) and Fig. 6(B), respectively. And the kinetics parameters were listed in Table 1. The pseudo-second-order model fitted the experimental data better due to the higher correlation coefficient (R^2). And the value of q_e ($2.47 \text{ mg}\cdot\text{g}^{-1}$) calculated by the pseudo-second-order is also more approximate to the experimental value ($2.23 \text{ mg}\cdot\text{g}^{-1}$), which indicates that the $\text{NH}_4^+\text{-N}$ adsorption process is mainly controlled by chemical adsorption (Wang et al., 2018).

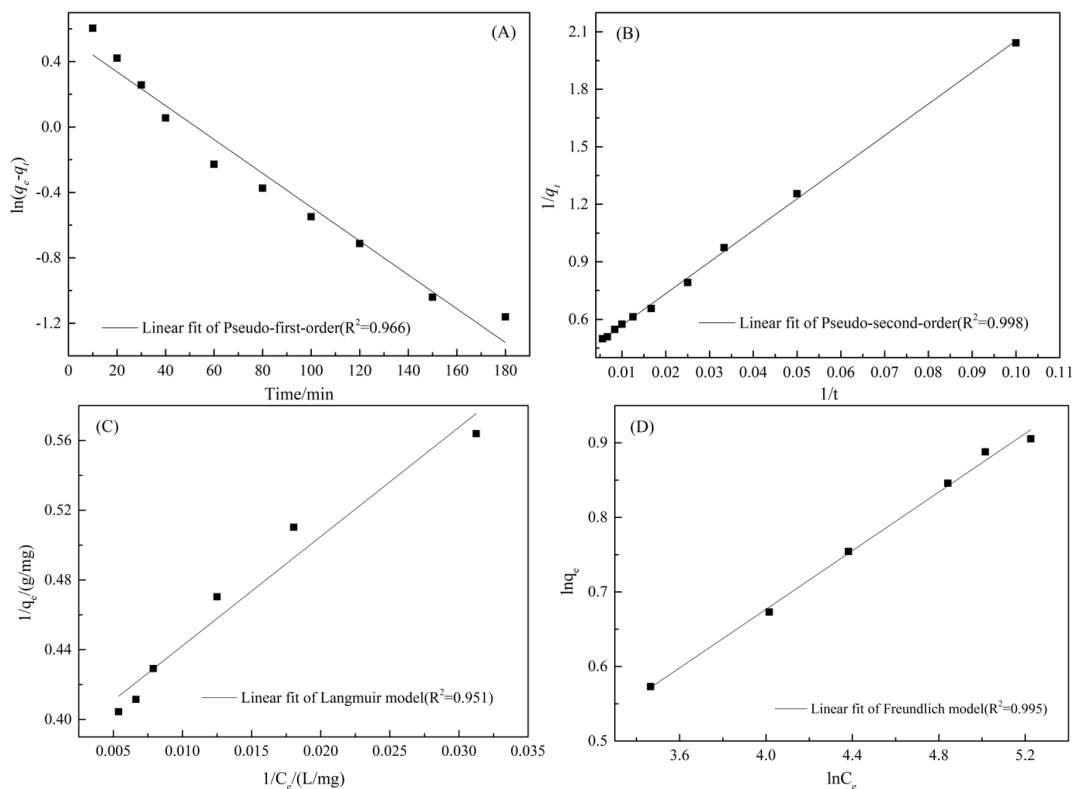


Fig. 6. Pseudo-first-order (A) and pseudo-second-order (B) kinetics, Langmuir isotherms (C) and Freundlich isotherms (D) for $\text{NH}_4^+\text{-N}$ adsorption on MgBC

The adsorption isotherms were fitted by Langmuir (Eq. (5)) and Freundlich (Eq. (6)) models, which were presented as follows:

$$\frac{1}{q_e} = \frac{1}{K_L q_{max} C_e} + \frac{1}{q_{max}} \quad (5)$$

where C_e ($\text{mg}\cdot\text{L}^{-1}$) is the equilibrium concentration of $\text{NH}_4^+\text{-N}$ in medium, q_e ($\text{mg}\cdot\text{g}^{-1}$) is the amount of $\text{NH}_4^+\text{-N}$ adsorbed on the MgBC, q_{max} ($\text{mg}\cdot\text{g}^{-1}$) is the maximum adsorption amount and K_L (L/mg) is a constant related to Langmuir model.

$$\ln q_e = \ln K_F + \frac{\ln C_e}{n} \quad (6)$$

where K_F ($\text{mg}^{(1-1/n)} \cdot \text{g}^{-1} \cdot \text{L}^{-1} / \text{n}$) is the Freundlich constant related to the adsorption capacity and n is a constant which feature the system.

The adsorption isotherms fitted by Langmuir and Freundlich methods were displayed in Fig. 6(C) and Fig. 6(D), respectively. And the adsorption isotherms parameters were listed in Table 2. The correlation coefficient obtained by Freundlich fitting was 0.995, higher than that of Langmuir model (0.951), indicating that Freundlich isotherm fitted better than Langmuir isotherm. Therefore, the NH_4^+ -N adsorption on MgBC is determined to be a homogenous and multilayer adsorption process. In addition, the value of n in Freundlich equation is calculated to be 0.197, which is in the range of 0.1~0.5, suggesting that the NH_4^+ -N can be easily adsorbed by MgBC.

3.2.3. Mechanism of NH_4^+ -N adsorption

XPS analysis was conducted to further investigate the mechanism of NH_4^+ -N adsorption on MgBC. Fig. 7(A) showed the survey spectra of MgBC before and after NH_4^+ -N adsorption. The main elements on the surface of MgBC were C, O, Mg, and Cl, which were consistent with the results obtained by EDS (Fig. 5(D)). The XPS intensities of Mg, O, and Cl were all diminished after adsorption process due to the dissolution of undecomposed MgCl_2 . And N element could be observed after adsorption process, indicating that NH_4^+ -N was successfully adsorbed on the surface. Fig. 7(B), Fig. 7(C), Fig. 7(D), Fig. 7(E) and Fig. 7(F) exhibited the high resolution spectra of C1s, O1s, Mg1s, P2p and N1s, respectively. The chemical environment of C (Fig. 7(B)) almost keep unchanged, revealing that the NH_4^+ -N could not be adsorbed on C of MgBC by chemical adsorption. According to the results from Fig. 7(C), the peaks at 532.9 eV and 530.6 eV were ascribed to C-O and Mg-O of MgBC and then disappeared after the adsorption process. The binding energy at 533.9 eV and 531.8 eV were ascribed to O=P and P-O- NH_4 adsorbed on MgBC, indicating that the PO_4^{3-} in basal medium can work as a "bridge" to further adsorb NH_4^+ -N. Fig. 7(D) showed the high resolution XPS spectra of Mg1s. The peak at 1305.3 eV corresponded to Mg-O, suggesting that Mg was existed as Mg-O before adsorption process. After the adsorption process, the peak Mg-O- NH_4 (1306.0 eV) and Mg-O-P (1304.7 eV) were observed, indicating that NH_4^+ -N and PO_4^{3-} could be adsorbed on MgBC. In addition, Fig. 7(E) and Fig. 7(F) can further confirm the adsorption of N and P on the surface of MgBC by comparison of the intensity of XPS spectra before and after adsorption process.

3.3. NH_4^+ -N removal characteristics of eluted water from weathered crust rare earth tailing

The eluted water was collected from weathered crust rare earth tailing with the NH_4^+ -N concentration of 94 mg/L. Fig. 8(A) exhibited the NH_4^+ -N removal efficiency after 5 h biodegradation under different pH ranging from 5.0 to 11.0 using MgBC (the blue), *P. fulva* (the red) and MgBC + *P. fulva* (the black), respectively. The NH_4^+ -N removal efficiency increased with the increasing pH in the range of 5~10 due to the elimination of competitive adsorption of H^+ . And then decreased because of the existing form of $\text{NH}_3 \cdot \text{H}_2\text{O}$ when the pH higher than 10. The optimum pH was 7.0 for *P. fulva* strain, which was in accordance with the results obtained in Fig. 2. The optimum pH for MgBC+*P. fulva* was chosen to be 7.0~8.0. As shown in Fig. 8(B), the NH_4^+ -N removal efficiency firstly increased to 21.6 % due to the chemical adsorption on MgBC in 3 h, and then removed via synergetic effect of *P. fulva* biodegradation and MgBC adsorption in the following time. And the consuming time for NH_4^+ -N removal was shorten to be 7 h due to the synergistic effect of MgBC and *P. fulva* strain. The nitrogen transformation characteristics in nitrogen removal process was shown in Fig. 8 (C). The NH_4^+ -N concentration decreased from 94.2 to 3.11 mg/L in 7.0 h, and NO_3^- -N was generated at 5~6 h due to the heterotrophic nitrification of *P. fulva* strain. NO_2^- -N was detected lower than 0.3 mg/L in the whole process. At 10.0 h, TN reached to the minimum concentration of 14.4 mg/L with a removal efficiency of 84.7 %. The SEM (Fig. 8 (D)) was carried out to investigated the microstructure of MgBC+*P. fulva*. The NH_4^+ -N could be adsorbed on the surface of MgBC, and *P. fulva* was also attached to the surface of MgBC, consuming the NH_4^+ -N adsorbed on MgBC and breaking the adsorption equilibrium. Thus, more NH_4^+ -N could be adsorbed on MgBC. The intensified effect for NH_4^+ -N removal was achieved by *P. fulva* and MgBC.

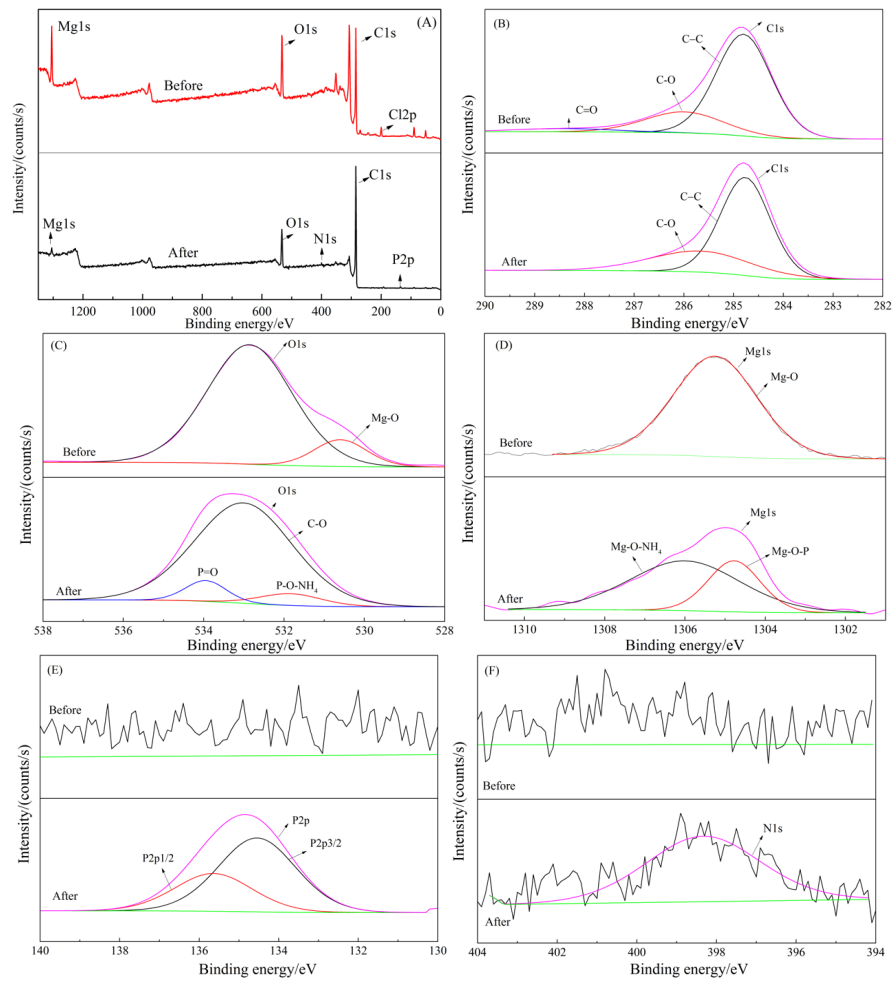


Fig. 7. XPS spectra of MgBC before and after adsorption; survey spectra(A); high resolution spectra of C1s(B), O1s(C), Mg1s(D), P2p(E), and N1s(F)

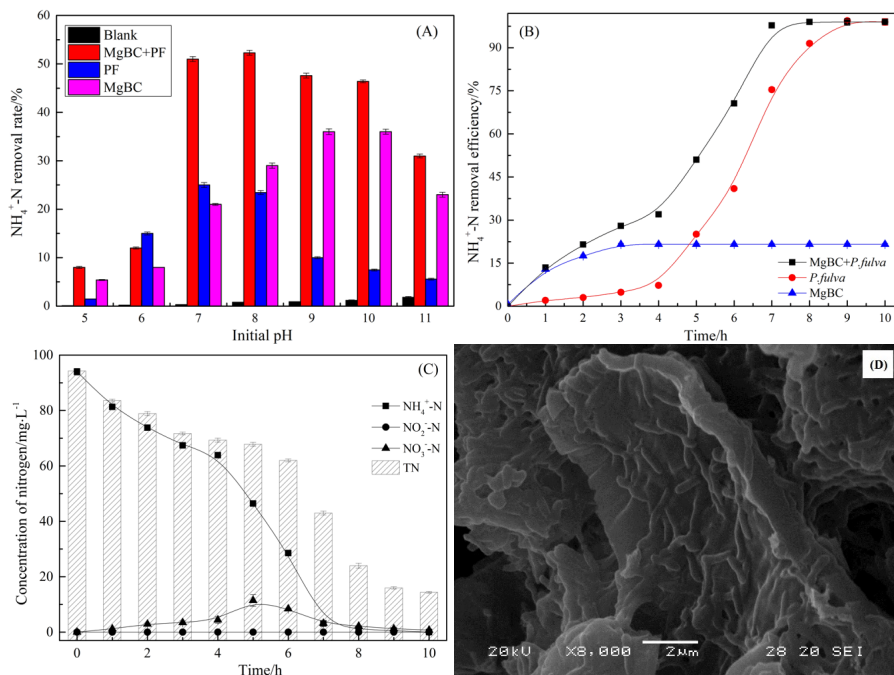


Fig. 8. The effect of pH (A) and time (B) on $\text{NH}_4^+\text{-N}$ removal using MgBC, *P. fulva* and MgBC+*P. fulva*, the nitrogen transformation characteristics (C), and microstructure of MgBC+*P. fulva* after $\text{NH}_4^+\text{-N}$ removal process

3.4. Mechanism of the intensified effect for NH_4^+ -N removal

According to the XPS and SEM results, intensified removal mechanism between MgBC and *P. fulva* was proposed in Fig. 9 (A). The MgBC provides a large amount of specific surface area for NH_4^+ -N adsorption and attachment sites for *P. fulva*. The NH_4^+ and PO_4^{3-} are adsorbed on the O and Mg, respectively. And NH_4^+ can be further attached to the O atom of PO_4^{3-} , which works as a “bridge” to adsorb more NH_4^+ on MgBC. The NH_4^+ can be immobilized on MgBC when the initial concentration is high and then released to system when its concentration gets lower due to the consuming of *P. fulva*, keeping a proper NH_4^+ concentration to facilitate the growth of *P. fulva* strain. The intensified effect for nitrogen removal can be achieved by the cooperation between MgBC and *P. fulva* strain.

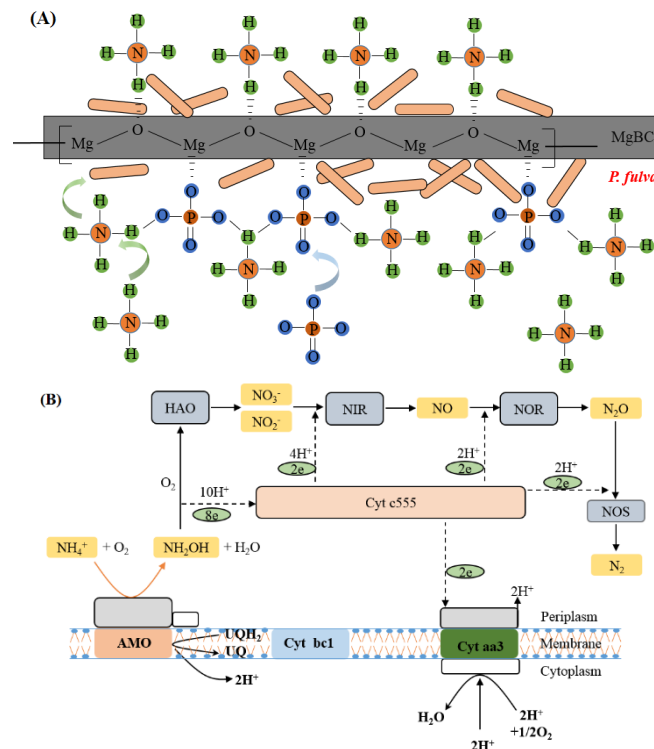


Fig. 9. Synergistic removal mechanism of MgBC in the presence of *P. fulva* strain (A), schematic diagram of the electron transport chain of *P. fulva*

The electron transport of chain of *P. fulva* is exhibited in Fig. 9 (B) according to the nitrogen transformation characteristics in experiments. Firstly, NH_4^+ -N is oxidized to NH_2OH in the presence of ammonia single oxidase (AMO), and NH_2OH can be further oxidized to NO_2^- -N and NO_3^- -N with the help of hydroxylamine oxidase (HAO). Then aerobic denitrification process occurs, reducing NO_2^- -N and NO_3^- -N to N_2 under serious enzymes such as nitrite reductase (NIR), nitrate reductase (NAR), nitric oxide reductase (NOR) and nitric oxide reductase (NOS). The NH_4^+ -N in eluted water from weathered crust rare earth tailing is successfully removed by the intensified effect of MgBC and *P. fulva* strain with great efficiency.

4. Conclusions

In summary, the isolated strain *P. fulva* and the as-prepared MgBC both have the ability of NH_4^+ -N removal. The effects of pH, temperature, initial NH_4^+ -N concentration on *P. fulva* biodegradation process were investigated, and the adsorption properties of MgBC was studied. The mechanism of the intensified effect of MgBC on *P. fulva* was revealed using XPS, BET, and SEM.

(1) The isolated *P. fulva* exhibited a rod-shaped morphology with an average length of 1.8 μm . NH_4^+ -N can be completely biodegraded under the optimal conditions of pH=7.0~8.0, temperature 30 $^\circ\text{C}$, and initial NH_4^+ -N concentration of 100 ~150 mg/L. The NH_4^+ -N tolerant concentration for *P.*

fulva was determined to be 300 mg/L, showing great feasibility for the treatment of eluted water from weathered crust rare earth tailing.

(2) The $\text{NH}_4^+\text{-N}$ adsorption properties of MgBC were studied. Pseudo-second-order model is more suitable to describe this adsorption kinetic with a higher correlation coefficient, and the Freundlich model fits the isotherm data well in adsorption process, implying that the adsorption of is a multilayer adsorption process mainly controlled by chemical adsorption. The mechanism of $\text{NH}_4^+\text{-N}$ adsorption was confirmed by XPS results. $\text{NH}_4^+\text{-N}$ was adsorbed to the O element of MgBC, and the PO_4^{3-} adsorbed on Mg element may act as a "bridge" to further adsorb the $\text{NH}_4^+\text{-N}$.

(3) The mechanism of the intensified effect between MgBC and *P. fulva* strain was revealed. The MgBC provides a large amount of specific surface area for $\text{NH}_4^+\text{-N}$ adsorption and attachment sites for *P. fulva*. The $\text{NH}_4^+\text{-N}$ can be immobilized on MgBC when the initial concentration is high and then released to system when its concentration gets lower due to the consuming of *P. fulva*, keeping a proper $\text{NH}_4^+\text{-N}$ concentration to facilitate the growth of *P. fulva* strain. The total nitrogen removal efficiency of the eluted weathered crust rare earth tailing reached 84.7 % using the complex of MgBC and *P. fulva*.

Acknowledgments

This work was financially supported by the National Key R&D Program of China (2018YFC1801800), the National Natural Science Foundation of China-Yunnan Joint Fund (U1802252), and the Scientific Research Foundation of Wuhan Institute of Technology (19QD58).

References

- AN, Q., ZHOU, Y., ZHAO, B., HUANG, X., 2020. Efficient ammonium removal through heterotrophic nitrification-aerobic denitrification by *Acinetobacter baumannii* strain AL-6 in the presence of Cr(VI). *J. Biosci. Bioeng.* 130, 622-629.
- AHMAD, M., LIU, S., MAHMOOD, N., MAHMOOD, A., ALI, M., ZHENG, M., NI, J., 2017. Effects of porous carrier size on biofilm development, microbial distribution and nitrogen removal in microaerobic bioreactors. *Bioresour. Technol.* 234, 360-369.
- BANERJEE, S., TIWADE, P. B., SAMBHAV, K., BANERJEE, C., BHAUMIK, S. K., 2019. Effect of alginate concentration in wastewater nutrient removal using alginate-immobilized microalgae beads: uptake kinetics and adsorption studies. *Biochem. Eng. J.* 149, 107241.
- CHEN, L., LIN, J., PAN, D., REN, Y., ZHANG, J., ZHOU, B., CHEN, L., LIN, J., 2020. Ammonium removal by a newly isolated heterotrophic nitrification-aerobic denitrification bacteria *Pseudomonas stutzeri* SDU10 and its potential in treatment of piggyery wastewater. *Curr. Microbiol.* 77, 2792-2801.
- CHEN, J., ZHAO, B., AN, Q., WANG, X., ZHANG, Y. X., 2016. Kinetic characteristics and modelling of growth and substrate removal by *Alcaligenes faecalis* strain NR. *Bioprocess Biosyst. Eng.* 39, 593-601.
- DUTTA, T., KIM, K., UCHIMIYA, M., KWON, E., JEON, B., DEEP, A., YUN, S., 2016. Global demand for rare earth resources and strategies for green mining. *Environ. Res.* 150, 182-190.
- FENG, J., ZHOU, F., CHI, R., LIU, X., XU, Y., LIU, Q., 2018. Effect of a novel compound on leaching process of weathered crust elution-deposited rare earth ore. *Miner. Eng.* 129, 63-70.
- GONG, B., WANG, Y., WANG, J., HUANG, W., ZHOU, J., HE, Q., 2018. Intensified nitrogen and phosphorus removal by embedding electrolysis in an anaerobic-anoxic-oxic reactor treating low carbon/nitrogen wastewater. *Bioresour. Technol.* 256, 562-565.
- HE, Z., ZHANG, Z., YU, J., XU, Z., XU, Y., ZHOU, F., CHI, R., 2016. Column leaching process of rare earth and aluminum from weathered crust elution-deposited rare earth ore with ammonium salts. *Trans. Nonferrous. Met. Soc. China.* 26, 3024-3033.
- HUANG, H., XIAO, X., YANG, L., YAN, B., 2010. Removal of ammonia nitrogen from washing wastewater resulting from the process of rare-earth elements precipitation by the formation of struvite. *Desalin. Water Treat.* 24, 85-92.
- HOU, J., XIA, L., MA, T., ZHANG, Y., ZHOU, Y., HE, X., 2017. Achieving short-cut nitrification and denitrification in modified intermittently aerated constructed wetland. *Bioresour. Technol.* 232, 10-17.
- HUANG, X., LI, W., ZHANG, D., QIN, W., 2013. Ammonium removal by a novel oligotrophic *Acinetobacter* sp. Y16 capable of heterotrophic nitrification-aerobic denitrification at low temperature. *Bioresour. Technol.* 146, 44-50.
- JIN, R., LIU, T., LIU, G., ZHOU, J., HUANG, J., WANG, A., 2015. Simultaneous heterotrophic nitrification and aerobic denitrification by the marine origin bacterium *Pseudomonas* sp. ADN-42. *Appl. Biochem. Biotechnol.* 175, 2000-2011.

- JIA, F., YANG, Q., LIU, X., LI, X., LI, B., ZHANG, L., PENG, Y., 2017. *Stratification of Extracellular Polymeric Substances (EPS) for Aggregated Anammox Microorganisms*. Environ. Sci. Technol. 51, 3260-3268.
- KIZITO, S., WU, S., KIRUI, W., LEI, M., LU, Q., BAH, H., DONG, R., 2015. *Evaluation of slow pyrolyzed wood and rice husks biochar for adsorption of ammonium nitrogen from piggery manure anaerobic digestate slurry*. Sci. Total. Environ. 505, 102-112.
- KOSUGI, Y., MATSUURA, N., LIANG, Q., YAMAMOTO-LKEMOTO, R., 2020. *Wastewater treatment using the "sulfate reduction, denitrification anammox and partial nitrification (SRDAPN)" process*. Chemosphere 256, 127092.
- LI, C., YANG, J., WANG, X., WANG, E., LI, B., HE, R., YUAN, H., 2015. *Removal of nitrogen by heterotrophic nitrification-aerobic denitrification of a phosphate accumulating bacterium Pseudomonas stutzeri YG-24*. Bioresour. Technol. 182, 18-25.
- LI, Q., ZHOU, L., ZHU, Y., QIN, L., 2017. *Prediction method for ammonia nitrogen pollution in the soil of ionic rare earth mine*. Environmental Impact Assessment 39, 56-59.
- LUO, H., SONG, Y., ZHOU, Y., YANG, L., ZHAO, Y., 2017. *Effects of rapid temperature rising on nitrogen removal and microbial community variation of anoxic/aerobic process for ABS resin wastewater treatment*. Environ. Sci. Pollut. Res. 24, 5509-5520.
- LU, T., YU, D., CHEN, G., WANG, X., HUANG, S., LIU, C., TANG, P., 2019. *NH₄⁺-N adsorption behavior of nitrifying sludge immobilized in waterborne polyurethane (WPU) pellets*. Biochem. Eng. J. 143, 196-201.
- LI, M., WEI, D., LIU, T., LIU, Y., YAN, L., WEI, Q., DU, B., XU, W., 2019. *EDTA functionalized magnetic biochar for Pb(II) removal: adsorption performance, mechanism and SVM model prediction*. Sep. Purif. Technol. 227, 115696.
- MA, W., HAN, Y., MA, W., HAN, H., ZHU, H., XU, C., LI, K., WANG, D., 2017. *Enhanced nitrogen removal from coal gasification wastewater by simultaneous nitrification and denitrification (SND) in an oxygen-limited aeration sequencing batch biofilm reactor*. Bioresour. Technol. 244, 84-91.
- PADHI, S. K., TRIPATHY, S., MOHANTY, S., MAITI, N. K., 2017. *Aerobic and heterotrophic nitrogen removal by Enterobacter cloacae CF-S27 with efficient utilization of hydroxylamine*. Bioresour. Technol. 232, 285-296.
- SHAMS, D. F., SINGHAL, N., ELEFSINIOTIS, P., 2018. *Effect of feed characteristics and operational conditions on treatment of dairy farm wastewater in a coupled anoxic-upflow and aerobic system*. Biochem. Eng. J. 133, 186-195.
- SU, J., CHENG, C., MA, F., 2017. *Comparison of the NH₄⁺-N removal ability by Klebsiella sp. FC61 in a bacterial suspension system and a bacterial immobilization system*. Sep. Purif. Technol. 172, 463-472.
- TALHA, M., GOSWAMI, M., GIRI, B. S., SHARMA, A., RAI, B. N., SINGH, R. S., 2018. *Bioremediation of Congo red dye in immobilized batch and continuous packed bed bioreactor by Brevibacillus parabrevis using coconut shell bio-char*. Bioresour. Technol. 252, 37-43.
- WANG, T., DANG, Q., LIU, C., YAN, J., FAN, B., CHA, D., YIN, Y., ZHANG, Y., 2016. *Heterotrophic nitrogen removal by a newly-isolated alkalitolerant microorganism, Serratia marcescens W5*. Bioresour. Technol. 211, 618-627.
- WANG, F., YU, J., ZHANG, Z., XU, Y., CHI, R., 2018. *An amino-functionalized ramie stalk-based adsorbent for highly effective Cu²⁺ removal from water: adsorption performance and mechanism*. Process. Saf. Environ. Protect. 117, 511-522.
- WU, X., ZHOU, F., LIU, C., FENG, J., ZHANG, Z., CHI, R., 2020. *Effect of polyacrylamide on the process of removing impurities in the rare earth leachate*. Physicochem. Probl. Miner. Process. 57(1):182-191.
- XIE, F., THIRI, M., WANG, H., 2021. *Simultaneous heterotrophic nitrification and aerobic denitrification by a novel isolated Pseudomonas mendocina X49*. Bioresour. Technol. 319, 124198.
- YANG, Y., LIU, Y., YANG, T., LV, Y., 2017. *Characterization of a microbial consortium capable of heterotrophic nitrifying under wide C/N range and its potential application in phenolic and coking wastewater*. Biochem. Eng. J. 120, 33-40.
- YUAN, Q., WANG, H., HANG, Q., DENG, Y., ZHENG, S., 2015. *Comparison of the MBBR denitrification carriers for advanced nitrogen removal of wastewater treatment plant effluent*. Environ. Sci. Pollut. Res. 22, 13970-13979.
- ZHANG, Z., HE, Z., YU, J., XU, Z., CHI, R., 2016. *Novel solution injection technology for in-situ leaching of weathered crust elution-deposited rare earth ores*. Hydrometallurgy 164, 248-256.
- ZHOU, F., FENG, J., SU, J., LIU, X., CHI, R., 2019. *Role of initial moisture content on the leaching process of weathered crust elution-deposited rare earth ores*. Sep. Purif. Technol. 217, 24-30.
- ZHAO, Z., QIU, Z., YANG, J., LU, S., CAO, L., ZHANG, W., XU, Y., 2017. *Recovery of rare earth elements from spent fluid catalytic cracking catalysts using leaching and solvent extraction techniques*. Hydrometallurgy 167, 183-188.
- ZHANG, Y., XIONG, Z., YANG, L., REN, Z., SHAO, P., SHI, H., XIAO, X., PAVLOSTATHIS, S., FANG, L., LUO, X., 2019. *Successful isolation of a tolerant co-flocculating microalgae towards highly efficient nitrogen removal in harsh rare earth element tailings (REEs) waste water*. Water Res. 166115076.

- ZHANG, D., SU, H., ANTWI, P., XIAO, L., LIU, Z., LI, J., 2019. *High-rate partial-nitritation and efficient nitrifying bacteria enrichment/out-selection via pH-DO controls: Efficiency, kinetics, and microbial community dynamics*. *Sci. Total Environ.* 692, 741-755.
- ZHANG, H., TANG, J., WANG, L., LIU, J., GURAV, R. G., SUN, K., 2016. *A novel bioremediation strategy for petroleum hydrocarbon pollutants using salt tolerant *Corynebacterium variabile* HRJ4 and biochar*. *J. Environ. Sci.* 47, 7-13.